MIR193BHG inhibits the proliferation, migration and invasion of trophoblasts by upregulating p53

PING WANG[1], YAN CHEN[2], SHUHENG YANG[3], JUNJUN GAO[1], ZHAN ZHANG[1] and HONG LI[2]

[1]Clinical Laboratory, The Third Affiliated Hospital of Zhengzhou University, Zhengzhou, Henan 450052, P.R. China; [2]Department of Obstetrics and Gynecology, The Third Affiliated Hospital of Zhengzhou University, Zhengzhou, Henan 450052, P.R. China; [3]Department of Cell Biology and Genetics, School of Basic Medical Sciences, Chongqing Medical University, Chongqing 400016, P.R. China

Received June 29, 2023; Accepted February 14, 2024

DOI: 10.3892/etm.2024.12609

Abstract. Aberrant expression of long non-coding RNAs (lncRNAs) serves a crucial role in the biological function of trophoblasts and contributes to preeclampsia (PE). lncRNA MIR193BHG expression is increased in PE placental tissues. In the present study, the effects of MIR193BHG on the function of trophoblasts were assessed to elucidate its underlying molecular mechanisms. The subcellular localization of MIR193BHG in HTR-8/SVneo human first-trimester extravillous trophoblast cells was determined using a fluorescent *in situ* hybridization assay and by conducting nucleocytoplasmic separation. The effect of MIR193BHG knockdown or overexpression on proliferation, migration, invasion and apoptosis was evaluated *in vitro* using Cell Counting Kit-8, wound healing, Transwell and flow cytometry assays. RNA-sequencing, Kyoto Encyclopedia of Genes and Genomes pathway enrichment analysis and protein-protein interaction network construction were subsequently performed to screen the downstream molecules regulated by MIR193BHG. Finally, rescue experiments were conducted to ascertain whether MIR193BHG influenced the biological function of trophoblasts via p53. MIR193BHG was predominantly localized in the nucleus of HTR-8/SVneo cells and overexpression of MIR193BHG significantly inhibited proliferation, migration and invasion, while increasing the rate of apoptosis of HTR-8/SVneo cells. Knockdown of MIR193BHG had the opposite effect. Furthermore, overexpression of MIR193BHG led to increases in both mRNA and protein levels of p53 compared with the control group, and knockdown of p53 rescued the effects induced by overexpression of MIR193BHG on cell proliferation, migration and invasion, while partially counteracting its effects on apoptosis of HTR-8/SVneo cells. In conclusion, the findings of the present study suggested that MIR193BHG served a critical role in progression of PE by regulating the expression of p53, and may be a novel therapeutic target for PE.

Correspondence to: Dr Zhan Zhang, Clinical Laboratory, The Third Affiliated Hospital of Zhengzhou University, 7 Kangfu Front Street, Zhengzhou, Henan 450052, P.R. China
E-mail: zhangzhanmmdd@163.com

Dr Hong Li, Department of Obstetrics and Gynecology, The Third Affiliated Hospital of Zhengzhou University, 7 Kangfu Front Street, Zhengzhou, Henan 450052, P.R. China
E-mail: lihongsfy@163.com

Key words: preeclampsia, MIR193BHG, long non-coding RNA, trophoblast, p53

Introduction

Preeclampsia (PE) is a pregnancy complication characterized by new-onset hypertension in pregnant patients following 20 weeks of gestation (1,2). PE occurs in 2-8% of all pregnancies worldwide, making it one of the leading causes of high maternal and neonatal morbidity and mortality (2). Despite extensive research (3-6), the etiology and pathogenesis of PE are incompletely understood. Placental dysfunction, particularly abnormal invasion and remodeling of maternal uterine spiral arteries by invasive extravillous trophoblast cells, is widely accepted to serve a critical role in the early stages of PE (7,8). Shallow invasion of trophoblasts into the endometrium and placental vascular recasting barriers leads to an insufficient oxygen supply, further leading to placental tissue ischemia, hypoxia and endothelial cell damage (7). Additionally, other potential molecular mechanisms such as oxidative stress, endoplasmic stress, inflammation and genetic factors have also been suggested (8). However, the exact molecular mechanisms underlying the role of trophoblast cells in PE progression are unclear.

Long non-coding RNAs (lncRNAs) are a class of RNA transcripts with no protein-coding capacity and >200 nucleotides in length (9,10). Studies have reported that lncRNAs can regulate gene expression and function at the epigenetic, transcriptional and post-transcriptional levels, while participating in numerous biological processes, such as cell differentiation, proliferation, apoptosis and invasion (11-14). lncRNAs have been implicated in numerous diseases such as cancer, diabetes, and neurodegenerative and cardiovascular diseases (13,15-18). Aberrantly expressed lncRNAs such as MALAT1, SNX17, SNHG14 and pseudogene HK2P1 have been identified in PE, and are involved in the pathogenesis of PE, potentially via regulation of angiogenesis, decidualization, inflammation and

immune regulation, proliferation, migration, and invasion of trophoblast cells (19-23). However, to the best of our knowledge, there is a lack of detailed studies on lncRNAs in PE and the functions and mechanisms of these lncRNAs.

MIR193BHG is located on human chromosome 16p13.12. A previous study reported that MIR193BHG expression is upregulated in placental tissue from patients with PE (24). Furthermore, hypoxia induces the expression of MIR193BHG in breast cancer cell lines (25). Overexpression of MIR193BHG inhibits breast cancer cell invasion and metastasis under both hypoxic and normoxic conditions; conversely, inhibition of MIR193BHG promotes cancer cell invasion and metastasis (25). Nevertheless, the effect of MIR193BHG on trophoblast cells in PE remains unclear. Therefore, the aim of the present study was to investigate the potential effects and underlying mechanisms of MIR193BHG on HTR-8/SVneo cells.

Materials and methods

Cell culture. The human first trimester extravillous trophoblast cell line (HTR-8/SVneo) was purchased from Wuhan Boster Biological Technology, Ltd. Cells were cultured in RPMI-1640 medium (HyClone; Cytiva) supplemented with 10% FBS (Zhejiang Tianhang Biotechnology Co., Ltd.). Cells were cultured at 37˚C in an atmosphere containing 5% CO_2 and used in further experiments during the logarithmic growth phase.

Cell transfection. MIR193BHG Smart Silencer and overexpression plasmids used to knock down (MIR193BHG-KD) and overexpress (MIR193BHG-OE) MIR193BHG as well as their negative controls (NCs) were synthesized by Guangzhou RiboBio Co., Ltd. The plasmid backbone was pEXP-RB-Mam-EGFP. The empty pEXP-RB-Mam-EGFP vector was used as the NC for overexpression (NC-OE). Smart Silencer is a mixture of three small interfering RNAs (siRNAs) and three antisense oligonucleotides (ASOs). The target sequences of the siRNAs were as follows: 5'-AAA CCTGCCAGTAATTTCAG-3', 5'-ATAAAAGGAGGCCTG CTTGG-3' and 5'-GCAAAGATGTTTCCAGAGA-3'. The target sequences of the ASOs were as follows: 5'-GAGCGT GTATAAAACCAAA-3', 5'-GCAACATGTTATTCTGAG TG-3' and 5'-GTGCTTCTGAACATTTGTT-3'. The Smart Silencer NC (NC-KD) did not contain domains homologous to humans, mice or rats (cat. no. lnc3N0000001-1-5). Three siRNAs specific for p53, as well as a non-targeting universal NC (NC-siRNA; cat. no. siN0000001-1-5), were synthesized by Guangzhou RiboBio Co., Ltd. The corresponding target sequences of p53 siRNA were as follows: p53-siRNA-1, 5'-GTACCACCATCCACTACAA-3'; p53-siRNA-2, 5'-AGA GAATCTCCGCAAGAAA-3' and p53-siRNA-3, 5'-GGAGTA TTTGGATGACAG-3'. Overexpression plasmids (2.5 μg), Smart Silencer (50 nM), siRNA (50 nM) or their respective NCs (2.5 μg, 50 and 50 nM, respectively) were transfected into HTR-8/SVneo cells using Lipofectamine® 3000 reagent (Invitrogen; Thermo Fisher Scientific, Inc.) in Opti-MEM Reduced Serum (Gibco; Thermo Fisher Scientific, Inc.) at 37˚C with 5% CO_2 for 48 h according to the manufacturer's instructions. At 48 h after transfection, the cells were collected for subsequent experiments.

RNA extraction and reverse transcription-quantitative PCR (RT-qPCR). Total RNA was extracted from HTR-8/SVneo cells using TRIzol® (Invitrogen; Thermo Fisher Scientific, Inc.) according to the manufacturer's protocol. The RNA was reverse-transcribed to cDNA using the ReverTra Ace qPCR RT kit (Toyobo Life Science) under the following conditions: 37˚C for 15 min, 50˚C for 5 min and 98˚C for 5 min. qPCR was performed using the SYBR Green Realtime PCR Master Mix (Toyobo Life Science) and an Applied Biosystems StepOne Real Time PCR system (Applied Biosystems; Thermo Fisher Scientific, Inc.). The following thermocycling conditions were used: Initial denaturation at 95˚C for 60 sec, followed by 40 cycles of 95˚C for 15 sec, 60˚C for 15 sec and 72˚C for 45 sec. The primers are listed in Table I. mRNA levels were quantified for each target gene using the $2^{-\Delta\Delta Cq}$ method (26), and normalized to GAPDH as an internal control.

Fluorescent in situ hybridization (FISH). FITC-labeled RNA probes for MIR193BHG were designed and synthesized by Shanghai QuiCell Biotechnology Co., Ltd. The MIR193BHG probe sequence was 5'-TCCAGCCGCAGCTCAATA AA-3'-FITC. FISH assays were performed using a Fluorescence *In Situ* Hybridization Kit for RNA (cat. no. R0306S; Beyotime Institute of Biotechnology). HTR-8/SVneo cells ($2.5x10^4$ cells/well) were seeded into a 24-well plate (Corning, Inc.) with sterile slides overnight. Cells were washed using 1X PBS for 5 min and fixed in 4% formaldehyde at room temperature for 10 min. Next, cells were washed twice with 1X PBS for 5 min each, after which cells were permeabilized in 1X PBS containing 0.5% Triton X-100 (Beyotime Institute of Biotechnology) for 5 min at 4˚C. After washing the cells with 1X PBS three times, they were blocked in pre-hybridization solution (hybridization solution containing 1% yeast RNA; cat. no. R0306S; Beyotime Institute of Biotechnology) at 37˚C for 30 min. Pre-hybridization solution was then discarded and cells were incubated with a hybridized mixture containing probe (1 μg/ml) at 37˚C overnight. Cells were sequentially washed in the dark at 42˚C for 5 min each with Washing Buffer I, II and III (cat. no. R0306S; Beyotime Institute of Biotechnology). After washing cells in 1X PBS for 5 min, they were stained with DAPI at room temperature for 5 min and washed with 1X PBS. The slides taken from the 24-well plate were then observed using a laser confocal microscope (magnification, x200). The entire process was protected against light to prevent quenching.

Nuclear and cytoplasmic RNA fractionation. A Cytoplasmic and Nuclear RNA Purification kit (Norgen Biotek Corp.) was used to isolate and purify both cytoplasmic and nuclear RNA from HTR-8/SVneo cells according to the manufacturer's instructions. RNA was subjected to RT-qPCR analysis as aforementioned. U6 is a type of small nuclear RNA and is stably expressed in the nucleus (27). U6 RNA was used as the nuclear control and GAPDH mRNA as the cytoplasmic control. The relative expression (%) of nuclear RNA=2^-nuclear Ct/(2^-cytoplasmic Ct + 2^-nuclear Ct). The relative expression (%) of cytoplasmic RNA=1-nuclear RNA (%).

Cell Counting Kit-8 (CCK-8) assays. Cell proliferation was detected using a CCK-8 assay kit (Dojindo Laboratories, Inc.) according to the manufacturer's instructions. Briefly,

Table I. Primer sequences for reverse transcription-quantitative PCR.

Gene	Sequence (5'-3')
MIR193BHG	F: AGGGGCTGATGAATTGAGGG
	R: TCAATGGCAGCAGGAGGTTA
p53	F: GAGGTTGGCTCTGACTGTACC
	R: TCCGTCCCAGTAGATTACCAC
U6	F: CTCGCTTCGGCAGCACA
	R: AACGCTTCACGAATTTGCGT
GAPDH	F: AGAACGGGAAGCTTGTCATC
	R: CATCGCCCCACTTGATTTTG

F, forward; R, reverse.

transfected HTR-8/SVneo cells were seeded into 96-well plates ($5x10^3$/well) with three replicates per group. At 0, 24, 48 and 72 h post-transfection, 10 μl CCK-8 working solution was dripped into each well and the cells were cultured for another 1 h at 37˚C. A microplate reader (Thermo Fisher Scientific, Inc.) was used to measure the optical density values at 450 nm.

Wound healing assay. At 24 h after transfection, HTR-8/SVneo cells were inoculated into a six-well plate and grown to 90-100% confluence. A 200-μl pipette tip was used to vertically scratch the bottom of the 6-well plate. The scratched cells were washed with PBS and incubated at 37˚C for 24 and 48 h in RPMI-1640 medium containing 2% FBS. Images were captured under an inverted light microscope. ImageJ software (version 1.51; National Institutes of Health) was used to quantify the wound closure. The percentage of wound closure was calculated as follows: Migration area (%)=(initial wound area-remaining wound area)/initial wound area x100.

Transwell assay. At 24 h post-transfection, cells were resuspended and adjusted to $2.5x10^4$ cells/ml using serum-free RPMI-1640 medium. Subsequently, 200 μl cell suspension was added into the upper chamber (8 μm; cat. no. 3422; Corning, Inc.), which was pre-coated with Matrigel (Corning, Inc.) at 37˚C for 1 h, and 500 μl RPMI-1640 medium containing 20% FBS was added into the lower chamber. Cells were incubated at 37˚C for 24 h. The invaded cells were fixed using 4% paraformaldehyde for 20 min at room temperature and stained with 0.1% crystal violet for 15 min at room temperature. The invaded cells were observed and counted manually in five random fields under a light microscope (Olympus Corporation).

Flow cytometry. Cell apoptosis was assessed using an Annexin V-FITC/PI kit (BD Biosciences). At 48 h post-transfection, HTR-8/SVneo cells were collected and resuspended with 500 μl precooled 1X binding buffer (including in the Annexin V-FITC/PI Apoptosis Detection Kit; BD Biosciences). Next, cells were double-stained in the dark with 5 μl Annexin V-FITC and PI (BD Biosciences) for 15 min at room temperature. Apoptosis including early apoptotic cells and late apoptotic cells, was determined within 1 h of staining using the DxFLEX flow cytometer (Beckman Coulter, Inc.) and analyzed using FlowJo software version 10.4 (FlowJo LLC).

Western blotting. Total proteins were extracted from HTR-8/SVneo cells using RIPA buffer (CoWin Biosciences) supplemented with 1% phenylmethanesulfonyl fluoride. The lysate was centrifuged at 10,000 x g for 10 min at 4˚C and the supernatant was collected. The total protein concentration was measured using the BCA protein assay kit (Thermo Fisher Scientific, Inc.). Equal amounts of protein (50 μg/lane) were separated by 10% SDS-PAGE and transferred to PVDF membranes. Following blocking with 5% non-fat milk in 1X Tris-buffered saline containing 0.1% Tween-20 (TBST) for 2 h at room temperature, membranes were incubated overnight with primary antibodies against p53 (1:2,000; cat. no. ab179477; Abcam) and GAPDH (1:4,000; cat. no. ab9485; Abcam) at 4˚C. Next, membranes were washed three times with TBST and incubated with horseradish peroxidase-conjugated goat anti-rabbit secondary antibody (1:10,000; cat. no. IH-0012; Beijing Dingguo Changsheng Biotechnology Co., Ltd.) for 1 h at room temperature. The bands were visualized using an ECL Plus Chemiluminescence Reagent kit (Beyotime Institute of Biotechnology) on an AI600 imaging system (Cytiva) to quantify their intensity. ImageJ software (version 1.51; National Institutes of Health) was used to quantify the relative protein expression. GAPDH was used as the loading control.

RNA-sequencing (RNA-seq) and computational analysis. HTR-8/SVneo cells transfected with MIR193BHG overexpression and empty plasmids were collected and lysed with TRIzol (CoWin Biosciences). The RNA concentration and quality were determined using a Qubit® 3.0 Fluorometer (Thermo Fisher Scientific, Inc.) and the Nanodrop One spectrophotometer (Thermo Fisher Scientific, Inc.). The integrity of total RNA was assessed using the Agilent 2100 Bioanalyzer (Agilent Technologies, Inc.), and samples with RNA integrity number values >7.0 were used for sequencing. Paired-end libraries were synthesized using the Stranded mRNA-seq Lib Prep Kit for Illumina (ABclonal Biotech Co., Ltd.) in accordance with the manufacturer's protocols. Briefly, the poly-A containing mRNA molecules were purified using poly-T oligo-attached magnetic beads. Following purification, the mRNA was fragmented into small pieces using divalent cations at 94˚C for 10 min. The cleaved RNA fragments were copied into first strand cDNA using reverse transcriptase and random primers. This was followed by second strand cDNA synthesis using DNA Polymerase I and RNase H. These cDNA fragments then underwent an end repair process, the addition of a single 'A' base and ligation of the adapters. The products were amplified by PCR and purified with magnetic beads (cat. no. RK20257; ABclonal Biotech Co., Ltd.) to create the final cDNA library according to the manufacturer's protocols of the mRNA-seq Lib Prep Kit for Illumina. Purified libraries were quantified using a Qubit® 3.0 Fluorometer (Thermo Fisher Scientific, Inc.) and validated using an Agilent 2100 bioanalyzer (Agilent Technologies, Inc.). The cluster was generated by cBot with the library diluted to 10 pM and then paired-end 150-bp sequencing was performed on the Illumina NovaSeq 6000 sequencing system (Illumina, Inc.) using the NovaSeq 6000 S4 Reagent kit v1.5 (cat. no. 20028312; Illumina, Inc.). cDNA

library construction and RNA sequencing were performed by Sinotech Genomics. The sequenced reads were then aligned to the human reference genome (GRCh38.91) using HISAT2 (version 2.1.0; https://daehwankimlab.github.io/hisat2/). Differential gene expression analysis was performed using EdgeR (version 3.30.3; Bioconductor). The threshold used to screen upregulated or downregulated mRNAs was $|\log_2(\text{fold change})|>0.5$ and $P<0.05$.

Kyoto Encyclopedia of Genes and Genomes (KEGG) enrichment analysis. After obtaining the differentially expressed genes, clusterProfiler (version 4.0.5; https://bioconductor.org/packages/clusterProfiler/) was used to perform the KEGG enrichment analysis in R software (version 4.1.0; https://www.r-project.org/). KEGG pathway enrichment (https://www.kegg.jp/kegg/kegg1.html) was used to identify the critical pathways that were closely related to MIR193BHG overexpression. $P<0.05$ was used to identify significant KEGG pathways. There was no gene count threshold.

Construction of the protein-protein interaction (PPI) network of differentially expressed genes. A PPI network of differentially expressed genes was constructed using the Search Tool for the Retrieval of Interacting Genes database (version 11.5; https://string-db.org/). Cytoscape (version 3.8.2; https://cytoscape.org/) was used to display the PPI network. Interactions with a combined score >0.4 were considered significant. The gene with the highest degree of connection to others was considered to be the hub gene, the associations of which were illustrated in Cytoscape.

Rescue assay. Rescue assays were performed to assess whether MIR193BHG affected viability, apoptosis, migration and invasion of HTR-8/SVneo cells by upregulating the expression of p53. HTR-8/SVneo cells were divided into three groups: MIR193BHG overexpression plasmid and p53-siRNA group, MIR193BHG overexpression plasmid and siRNA NC group, and empty plasmid and siRNA NC group.

Statistical analysis. Data from three independent replicates are presented as the mean ± standard deviation. SPSS 21.0 (IBM Corp.) was used to perform statistical analysis. Two group comparisons were conducted using the unpaired two-tailed Student's t-test and multiple group comparisons were performed using one-way ANOVA followed by Bonferroni's post hoc test. $P<0.05$ was considered to indicate a statistically significant difference.

Results

MIR193BHG inhibits proliferation and promotes apoptosis of trophoblast cells. HTR-8/SVneo cells were transfected with MIR193BHG overexpression or empty plasmids and the transfection efficiency was confirmed by RT-qPCR. The results indicated that the MIR193BHG overexpression vector significantly increased the levels of MIR193BHG compared with the NC (Fig. 1A). The levels of MIR193BHG were significantly decreased in HTR-8/SVneo cells following transfection with the MIR193BHG Smart Silencer compared with the control (Fig. 1B).

To assess the role of MIR193BHG in HTR-8/SVneo cells, a CCK-8 assay was performed. There was a significant decrease in cell proliferation at 24, 48 and 72 h in the MIR193BHG-OE group compared with the NC-OE group (Fig. 1C). Conversely, knockdown of MIR193BHG resulted in a significant increase in cell proliferation at 24, 48 and 72 h compared with the NC-KD group (Fig. 1D).

Flow cytometry demonstrated that the apoptosis rate of HTR-8/SVneo cells was significantly higher in the MIR193BHG-OE group compared with the NC-OE group (Fig. 1E). The apoptosis rate was significantly lower in the MIR193BHG-KD group compared with the NC-KD group (Fig. 1F).

MIR193BHG inhibits trophoblast cell migration and invasion. The invasion and migration of trophoblasts are key for placentation, with dysregulation serving a critical role in the pathogenesis of PE (28,29). Therefore, wound healing and Transwell assays were performed to assess the migration and invasion of HTR-8/SVneo cells in response to MIR193BHG overexpression and knockdown. The percentage of wound closure was significantly decreased in the MIR193BHG-OE group compared with the NC-OE group at 24 and 48 h (Fig. 2A), as was the number of invaded cells at 24 h (Fig. 2C). Conversely, the percentage of wound closure was significantly increased at 48 h in the MIR193BHG-KD group compared with the NC-KD group (Fig. 2B), as was the number of invaded cells at 24 h (Fig. 2D).

MIR193BHG upregulates p53 expression in HTR-8/SVneo cells. Using FISH and cell fractionation assays, it was demonstrated that MIR193BHG was predominantly localized in the nucleus (~60%) (Fig. 3A and B), suggesting it may participate in the transcriptional regulation processes. To assess downstream molecules and signaling pathways regulated by MIR193BHG, RNA-seq was conducted in the MIR193BHG overexpression and control groups. This demonstrated that 63 mRNAs were upregulated and 84 mRNAs were downregulated in the MIR193BHG overexpression group compared with the control group (Fig. 3C and D). KEGG pathway analysis demonstrated that the differentially expressed genes were primarily enriched in 'cellular senescence', 'cell cycle', 'fluid shear stress and atherosclerosis' and 'p53 signaling pathway' (Fig. 3E). Notably, p53 emerged as a hub gene within the PPI network constructed based on differentially expressed mRNAs (Fig. 3F), suggesting its potential role as a downstream molecule regulated by MIR193BHG.

RT-qPCR demonstrated a significant increase in the levels of p53 mRNA in the MIR193BHG overexpression group compared with the control group (Fig. 3G). Western blotting also demonstrated increased protein expression of p53 in the MIR193BHG overexpression group, which corroborated the findings of RNA-seq analysis (Fig. 3H).

Silencing of p53 attenuates the effects of MIR193BHG on HTR-8/SVneo cells. To assess whether MIR193BHG affects viability, apoptosis, migration and invasion of HTR-8/SVneo cells by upregulating the expression of p53, rescue assays were performed. RT-qPCR demonstrated that the mRNA expression levels of p53 in HTR-8/SVneo cells were significantly

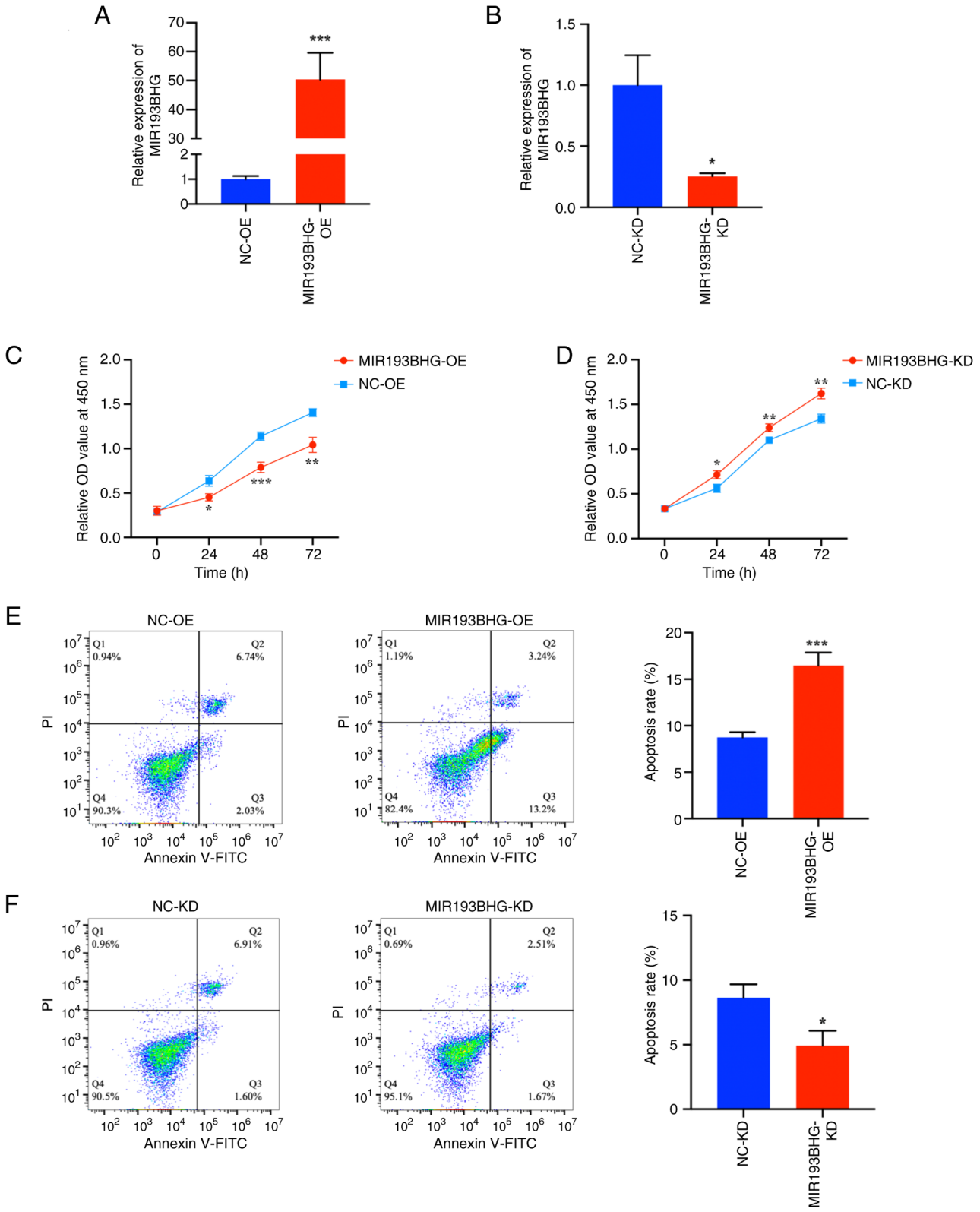

Figure 1. MIR193BHG inhibits trophoblast proliferation and promotes apoptosis *in vitro*. Reverse transcription-quantitative PCR analysis of MIR193BHG expression in HTR-8/SVneo cells following MIR193BHG (A) OE and (B) KD. Cell Counting Kit-8 assays showing the proliferation of HTR-8/SVneo cells following MIR193BHG (C) OE and (D) KD at 24, 48 and 72 h. Flow cytometry showing apoptosis of HTR-8/SVneo cells following MIR193BHG (E) OE and (F) KD. *P<0.05, **P<0.01 and ***P<0.001 vs. NC. OD, optical density; KD, knockdown; OE, overexpression; NC, negative control; NC-OE, empty vector; NC-KD, Smart Silencer negative control.

downregulated following transfection with p53-siRNA-1, p53-siRNA-2 and p53-siRNA-3 compared with NC-siRNA. A decrease in p53 protein levels was also demonstrated by western blotting following transfection with p53-siRNA-1, p53-siRNA-2 and p53-siRNA-3. Furthermore, the knock-down efficiency of p53-siRNA-3 was relatively high, and

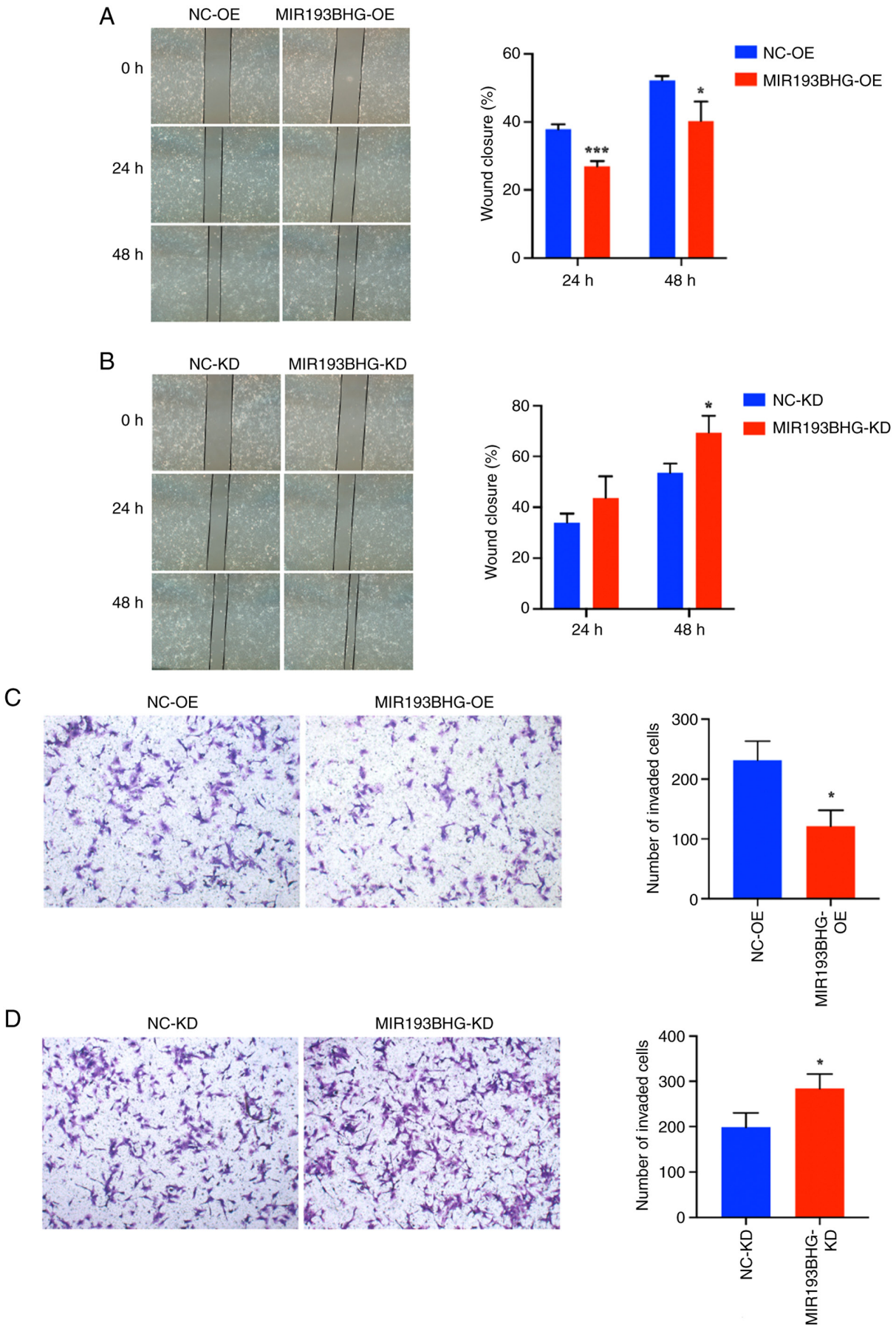

Figure 2. MIR193BHG inhibits trophoblast cell migration and invasion. Wound healing assay measuring migration of HTR-8/SVneo cells following MIR193BHG (A) OE and (B) KD (magnification, x40). Transwell assay showing invasion of HTR-8/SVneo cells following MIR193BHG (C) OE and (D) KD (magnification, x100). *P<0.05 and ***P<0.001 vs. NC. KD, knockdown; OE, overexpression. NC, negative control; NC-OE, empty vector; NC-KD, Smart Silencer negative control.

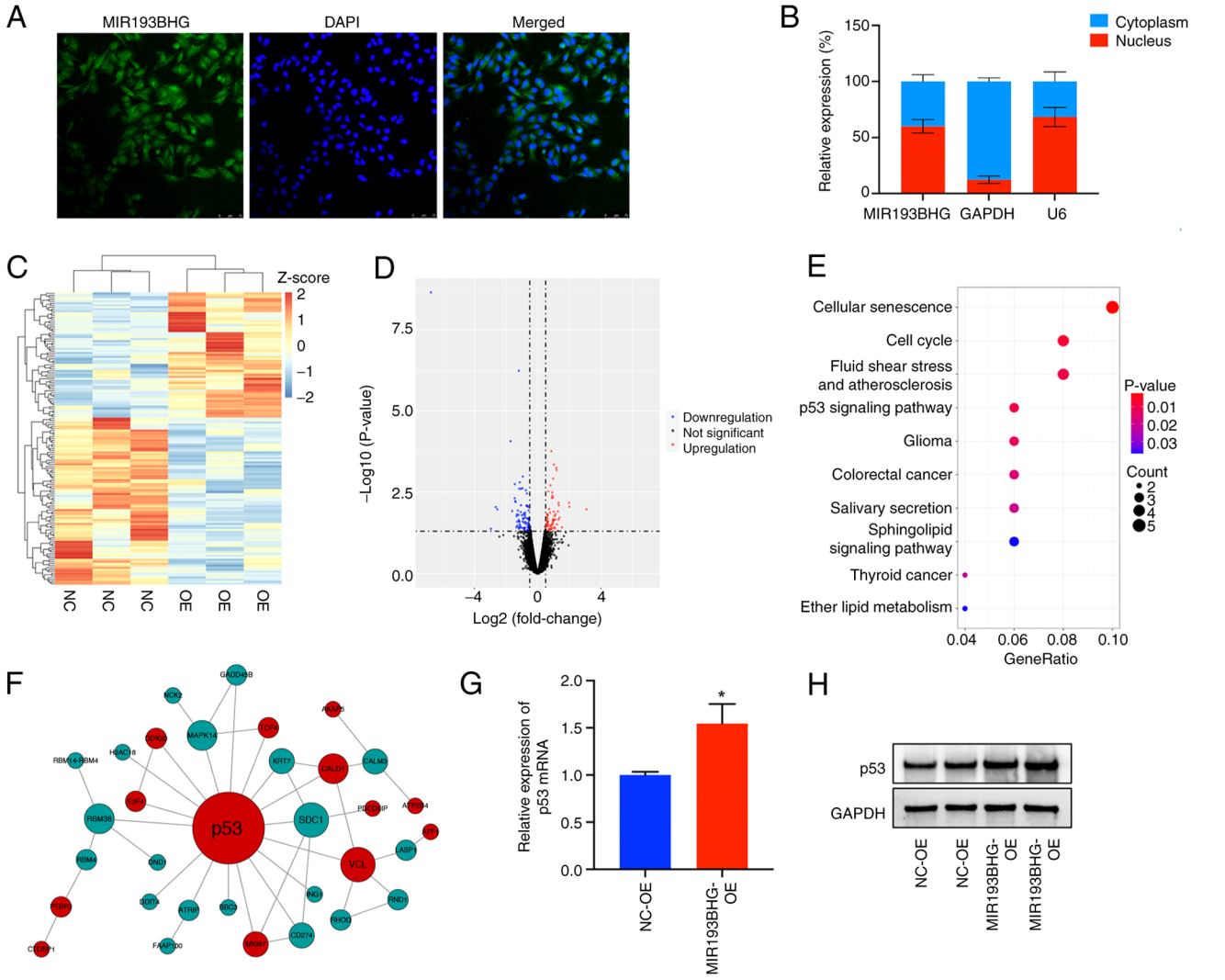

Figure 3. MIR193BHG upregulates expression of p53 in HTR-8/SVneo cells. (A) Fluorescence *in situ* hybridization assay demonstrating subcellular localization of MIR193BHG in HTR-8/SVneo cells (magnification, x200). (B) Subcellular localization of MIR193BHG in HTR-8/SVneo cells. U6 and GAPDH were used as internal controls. (C) Heatmap and (D) volcano plot showing differentially expressed genes in HTR-8/SVneo cells transfected with MIR193BHG overexpression plasmids vs. control vector. (E) Top 10 enriched KEGG pathways following MIR193BHG overexpression in HTR-8/SVneo cells. P<0.05 was used to identify significant KEGG pathways. (F) PPI network of differentially expressed genes showing that p53 was the hub gene. The node size is proportional to the degree of connectivity of the node. Red represents upregulated genes, while green represents downregulated genes. (G) Reverse transcription-quantitative PCR analysis of p53 mRNA expression in HTR-8/SVneo cells following MIR193BHG overexpression. (H) Expression levels of p53 protein were assessed by western blotting in HTR-8/SVneo cells overexpressing MIR193BHG. *P<0.05 vs. NC-OE. KEGG, Kyoto Encyclopedia of Genes and Genomes; OE, overexpression; NC, negative control; NC-OE, empty vector.

thus, p53-siRNA-3 was used for subsequent experiments (Fig. 4A and B).

The CCK-8 assay demonstrated that the viability of HTR-8/SVneo cells was decreased at 24, 48 and 72 h in the MIR193BHG overexpression group compared with the control group, whereas co-transfection of MIR193BHG and p53-siRNA-3 partially reduced this effect (Fig. 4C). Flow cytometry demonstrated that the apoptosis rate of HTR-8/SVneo cells was significantly higher in the MIR193BHG overexpression group compared with the control group, whereas co-transfection of MIR193BHG and p53-siRNA-3 partially counteracted the apoptotic effects induced by MIR193BHG in HTR-8/SVneo cells (Fig. 4D). The percentage of wound closure (Fig. 4E) and the number of invaded cells (Fig. 4F) were significantly decreased in the MIR193BHG overexpression group compared with the control group at 24 h, and this repression was partially reversed by co-transfection of MIR193BHG and p53-siRNA-3.

Discussion

PE is a leading cause of high maternal and neonatal morbidity and mortality worldwide (2). However, its etiology and pathogenesis remain unclear, with no effective preventive and therapeutic measures currently available. lncRNAs are aberrantly expressed in numerous types of disease, including cancer (30), cardiovascular disease (31), neurodegenerative diseases (32) and diabetic nephropathy (33). Previous studies have highlighted the association between lncRNAs and trophoblast cell function in PE (16,34,35). A previous study reported that MIR193BHG was highly expressed in the placenta in PE and exhibited robust performance in differentiating patients

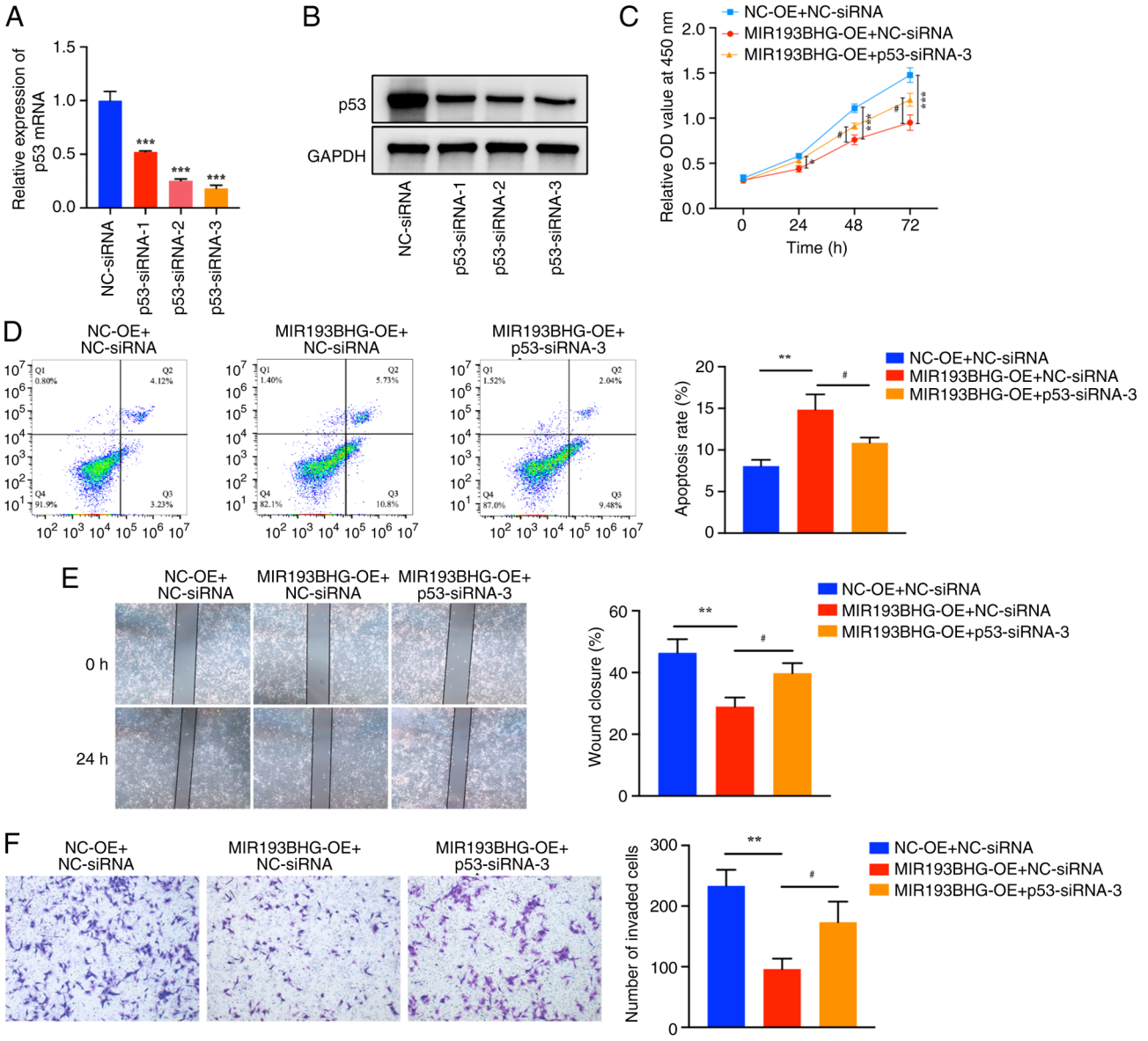

Figure 4. Silencing of p53 attenuates the effects of MIR193BHG on HTR-8/SVneo cells. HTR-8/SVneo cells were divided into three groups (MIR193BHG-OE + p53-siRNA-3, MIR193BHG-OE + NC-siRNA and NC-OE + NC-siRNA), after which rescue experiments were performed. (A) Reverse transcription-quantitative PCR and (B) western blotting were performed to examine mRNA and protein expression levels of p53, respectively, following transfection with p53-siRNA-1, p53-siRNA-2 and p53-siRNA-3. ***P<0.001 vs. NC-siRNA. (C) Cell proliferation was measured using a Cell Counting Kit-8 assay and (D) flow cytometry was used to detect apoptosis. (E) Wound healing assays were used to examine cell migration (magnification, x40). (F) A Transwell invasion assay was used to examine cell invasion (magnification, x100). *P<0.05, **P<0.01 and ***P<0.001 vs. NC-OE + NC-siRNA; #P<0.05 vs. MIR193BHG-OE + NC-siRNA. OE, overexpression; NC, negative control; siRNA, small interfering RNA; OD, optical density; NC-OE, empty vector; NC-siRNA, non-targeting siRNA negative control.

with preeclampsia from healthy controls (24). Furthermore, upregulation of MIR193BHG has been reported in the serum of patients with PE, with its expression levels associated with disease severity (36). Therefore, MIR193BHG is suggested to serve a role in the development, early diagnosis and treatment of PE.

In the present study, overexpression of MIR193BHG significantly inhibited proliferation, invasion and migration, while increasing the apoptosis rate of HTR-8/SVneo cells. Conversely, knockdown of MIR193BHG had the opposite effects. Wu *et al* (25) reported that knockdown of MIR193BHG in MDA-MB-231 cells promoted invasion and viability; however, overexpression of MIR193BHG inhibited invasion. This finding was consistent with the present study, suggesting that highly expressed MIR193BHG may be involved in the development of PE via inhibition of the biological function of trophoblast cells.

The function of lncRNAs primarily relies on their subcellular localization. Studies have reported that most lncRNAs are located in the nucleus and participate in gene regulation at the epigenetic and transcriptional levels, such as chromatin remodeling, histone modification and DNA methylation, primarily via interaction with DNA, RNA or proteins (37,38). Cytoplasmic lncRNAs regulate gene expression mostly at the post-transcriptional level by regulating mRNA stability, altering mRNA translation efficiency, serving as microRNA

(miRNA) precursors or competing with miRNA-mediated repression to regulate gene expression (39,40). The findings of the present study indicated that MIR193BHG was primarily localized in the nucleus, suggesting its potential involvement in transcriptional regulation.

RNA-seq was performed to assess the downstream targets of MIR193BHG. *In vitro* experiments demonstrated upregulation of both mRNA and protein levels of p53 following overexpression of MIR193BHG. The p53 gene, located on chromosome 17q13.1, encodes the p53 protein and serves as a key tumor suppressor gene involved in tumorigenesis (41). Additionally, p53 can regulate a large number of genes associated with cellular senescence, cell cycle progression, apoptosis and DNA repair (42). p53 expression is increased in placental tissues, HUVECs and maternal serum in PE (43,44). Elevated levels of p53 in trophoblasts have been reported to inhibit cell viability, proliferation, migration and invasion, while increasing the levels of apoptosis (45). This leads to cell cycle arrest and contributes to the development of PE (46). Gao *et al* (44) reported that p53 expression in HUVECs isolated and cultured from PE pregnancies was increased, along with suppressed cell proliferation characterized by increased G_1 arrest and apoptosis. Furthermore, decreased expression of protein disulfide isomerase family A member 3 (PDIA3) induces trophoblast apoptosis and suppresses trophoblast proliferation by regulating the mouse double minute 2 (MDM2)/p53/p21 signaling pathway in PE (47). Additionally, downregulation of lumican in the placental tissues of PE may also be involved in PE via inhibition of Bcl-2 expression as well as promotion of p53 expression (48).

Furthermore, lncRNAs serve roles in the p53 regulatory network, and thus, participate in the occurrence and development of certain types of diseases (42,49). In colon cancer, the overexpression of lncRNA RNA component of mitochondrial RNA-processing endoribonuclease inhibits p53 activity by promoting MDM2-induced p53 ubiquitination and degradation, thereby promoting proliferation of colorectal cancer cells in a p53-dependent manner (50). In renal cell carcinoma, the lncRNA activated by TGF-β inhibits the expression of p53 by binding to DNA methyltransferase 1, which leads to an increase in proliferation and migration of renal carcinoma cells as well as a decrease in apoptosis (51). Additionally, lncRNA growth arrest specific 5 acts as a negative regulator of vascular smooth muscle survival in vascular remodeling by directly binding to p53 and p300, stabilizing p53-p300 interaction and regulating vascular smooth muscle cell survival by inducing p53 downstream target genes (52). Knockdown of lncRNA maternally expressed gene 3 protects the heart against apoptosis induced by endoplasmic reticulum stress by targeting p53 (53).

To the best of our knowledge, no studies have elucidated the involvement of lncRNAs in the pathogenesis of PE by regulating p53. Furthermore, to the best of our knowledge, no research has been conducted on regulation of p53 expression mediated by MIR193BHG. By constructing a PPI network of differentially expressed mRNAs identified using RNA-seq, the present study identified p53 as the hub gene. The KEGG pathway enrichment analysis also demonstrated that the significantly enriched pathways of the differentially expressed genes included 'cellular senescence', 'cell cycle', 'fluid shear stress and atherosclerosis' and the 'p53 signaling pathway'. These pathways have all been confirmed to be related to p53 (54,55). Therefore, it was suggested that p53 may serve as a downstream molecule of MIR193BHG. Subsequently, expression levels of p53 mRNA and protein were verified by RT-qPCR and western blotting following overexpression of MIR193BHG, which yielded consistent results with those obtained by RNA-seq. Notably, overexpression of MIR193BHG led to an increase in p53 mRNA and protein expression. Given that p53 is hypothesized to serve a role in the pathogenesis of PE, evaluating whether MIR193BHG can affect behavior of trophoblasts by regulating the expression of p53 could enhance the understanding of the underlying mechanisms involved in PE. Consequently, co-transfection experiments involving both p53-siRNA and MIR193BHG overexpression plasmids were conducted using HTR-8/SVneo cells to evaluate whether knockdown of p53 could reverse changes in trophoblast behavior caused by MIR193BHG overexpression. Knockdown of p53 partially restored the function of trophoblasts via modulation of p53 expression, thus highlighting the involvement of p53 in the pathogenic mechanism underlying PE.

The present study preliminarily assessed the pathogenesis of MIR193BHG in PE and provided an experimental basis for subsequent research. However, certain limitations exist within the present study. Firstly, it is necessary to confirm expression patterns and localization of p53 *in vivo* through immunohistochemistry using clinical specimens to validate these conclusions. Additionally, the precise mechanism by which MIR193BHG regulates the expression of p53 remains unknown. Subsequent experiments should use chromatin immunoprecipitation assays, RNA pulldown, RNA immunoprecipitation assays and other techniques to assess whether MIR193BHG directly binds to p53 or indirectly regulates p53 expression through alternative mechanisms.

Finally, the present study primarily focused on evaluating the impact of MIR193BHG on the biological functions of extravillous trophoblastic cells. However, as the placenta contains stromal components such as fibroblasts and vascular endothelial cells, as well as blood components, including inflammatory cells such as lymphocytes and macrophages, the effects of MIR193BHG on other types of placental cells should be explored in future studies. These investigations may provide additional insights into the involvement of MIR193BHG in the pathogenesis of PE.

To the best of our knowledge, the present study was the first to demonstrate that lncRNA MIR193BHG upregulated p53 expression and influenced the biological behaviors of HTR-8/SVneo cells in PE. The findings of the present study may provide a novel diagnostic and therapeutic target for PE.

Acknowledgements

Not applicable.

Funding

The present study was supported by the Medical Science and Technology Research Plan of Henan Province in 2019 (grant no. LHGJ20190356).

Availability of data and materials

The data generated in the present study may be found in the Gene Expression Omnibus database under accession number GSE245279 or at the following URL: https://www.ncbi.nlm.nih.gov/geo/query/acc.cgi?acc=GSE245279. The other data generated in the present study may be requested from the corresponding author.

Authors' contributions

HL and ZZ designed the study. PW, YC and SY performed experiments and conducted the data analysis. JG performed bioinformatics analysis. PW wrote the manuscript and JG revised the manuscript critically for important intellectual content. PW, HL, ZZ and JG confirm the authenticity of all the raw data. All authors have read and approved the final manuscript.

Ethics approval and consent to participate

Not applicable.

Patient consent for publication

Not applicable.

Competing interests

The authors declare that they have no competing interests.

References

1. Chappell LC, Cluver CA, Kingdom J and Tong S: Pre-eclampsia. Lancet 398: 341-354, 2021.
2. No authors listed: Gestational hypertension and preeclampsia: ACOG practice bulletin summary, number 222. Obstet Gynecol 135: 1492-1495, 2020.
3. Jung E, Romero R, Yeo L, Gomez-Lopez N, Chaemsaithong P, Jaovisidha A, Gotsch F and Erez O: The etiology of preeclampsia. Am J Obstet Gynecol 226 (2S): S844-S866, 2022.
4. Cooke WR, Jiang P, Ji L, Bai J, Jones GD, Lo YMD, Redman C and Vatish M: Differential 5'-tRNA fragment expression in circulating preeclampsia syncytiotrophoblast vesicles drives macrophage inflammation. Hypertension 81: 876-886, 2024.
5. Wang J, Gao Y, Ren S, Li J, Chen S, Feng J, He B, Zhou Y and Xuan R: Gut microbiota-derived trimethylamine N-Oxide: A novel target for the treatment of preeclampsia. Gut Microbes 16: 2311888, 2024.
6. Li Y, Sang Y, Chang Y, Xu C, Lin Y, Zhang Y, Chiu PCN, Yeung WSB, Zhou H, Dong N, *et al*: A galectin-9-driven CD11c^{high} decidual macrophage subset suppresses uterine vascular remodeling in preeclampsia. Circulation 149: 1670-1688, 2024.
7. Jim B and Karumanchi SA: Preeclampsia: Pathogenesis, prevention, and long-term complications. Semin Nephrol 37: 386-397, 2017.
8. Hod T, Cerdeira AS and Karumanchi SA: Molecular mechanisms of preeclampsia. Cold Spring Harb Perspect Med 5: a023473, 2015.
9. Stein LD: Human genome: End of the beginning. Nature 431: 915-916, 2004.
10. Djebali S, Davis CA, Merkel A, Dobin A, Lassmann T, Mortazavi A, Tanzer A, Lagarde J, Lin W, Schlesinger F, *et al*: Landscape of transcription in human cells. Nature 489: 101-108, 2012.
11. Dhaka B, Zimmerli M, Hanhart D, Moser MB, Guillen-Ramirez H, Mishra S, Esposito R, Polidori T, Widmer M, García-Pérez R, *et al*: Functional identification of cis-regulatory long noncoding RNAs at controlled false discovery rates. Nucleic Acids Res 52: 2821-2835, 2024.
12. Sun N, Qin S, Zhang L and Liu S: Roles of noncoding RNAs in preeclampsia. Reprod Biol Endocrinol 19: 100, 2021.
13. Liu SJ, Dang HX, Lim DA, Feng FY and Maher CA: Long noncoding RNAs in cancer metastasis. Nat Rev Cancer 21: 446-460, 2021.
14. Zhang Y, He XY, Qin S, Mo HQ, Li X, Wu F, Zhang J, Li X, Mao L, Peng YQ, *et al*: Upregulation of PUM1 expression in preeclampsia impairs trophoblast invasion by negatively regulating the expression of the lncRNA HOTAIR. Mol Ther 28: 631-641, 2020.
15. Ponting CP, Oliver PL and Reik W: Evolution and functions of long noncoding RNAs. Cell 136: 629-641, 2009.
16. McAninch D, Roberts CT and Bianco-Miotto T: Mechanistic insight into long noncoding RNAs and the placenta. Int J Mol Sci 18: 1371, 2017.
17. Statello L, Guo CJ, Chen LL and Huarte M: Gene regulation by long non-coding RNAs and its biological functions. Nat Rev Mol Cell Biol 22: 96-118, 2021.
18. Mirzadeh Azad F, Polignano IL, Proserpio V and Oliviero S: Long noncoding RNAs in human stemness and differentiation. Trends Cell Biol 31: 542-555, 2021.
19. Wu HY, Wang XH, Liu K and Zhang JL: LncRNA MALAT1 regulates trophoblast cells migration and invasion via miR-206/IGF-1 axis. Cell Cycle 19: 39-52, 2020.
20. Guiyu S, Quan N, Ruochen W, Dan W, Bingnan C, Yuanyua L, Yue B, Feng J, Chong Q and Leilei W: LncRNA-SNX17 promotes HTR-8/SVneo proliferation and invasion through miR-517a/IGF-1 in the placenta of diabetic macrosomia. Reprod Sci 29: 596-605, 2022.
21. Zhang Y and Zhang M: lncRNA SNHG14 involved in trophoblast cell proliferation, migration, invasion and epithelial-mesenchymal transition by targeting miR-330-5p in preeclampsia. Zygote 29: 108-117, 2021.
22. Lv H, Tong J, Yang J, Lv S, Li WP, Zhang C and Chen ZJ: Dysregulated pseudogene HK2P1 may contribute to preeclampsia as a competing endogenous RNA for hexokinase 2 by impairing decidualization. Hypertension 71: 648-658, 2018.
23. Li X, Song Y, Liu F, Liu D, Miao H, Ren J, Xu J, Ding L, Hu Y, Wang Z, *et al*: Long non-coding RNA MALAT1 promotes proliferation, angiogenesis, and immunosuppressive properties of mesenchymal stem cells by inducing VEGF and IDO. J Cell Biochem 118: 2780-2791, 2017.
24. Zhang Z, Wang P, Zhang L, Huang C, Gao J, Li Y and Yang B: Identification of key genes and long noncoding RNA-associated competing endogenous RNA (ceRNA) networks in early-onset preeclampsia. Biomed Res Int 2020: 1673486, 2020.
25. Wu X, Niculite CM, Preda MB, Rossi A, Tebaldi T, Butoi E, White MK, Tudoran OM, Petrusca DN, Jannasch AS, *et al*: Regulation of cellular sterol homeostasis by the oxygen responsive noncoding RNA lincNORS. Nat Commun 11: 4755, 2020.
26. Livak KJ and Schmittgen TD: Analysis of relative gene expression data using real-time quantitative PCR and the 2(-Delta Delta C(T)) method. Methods 25: 402-408, 2001.
27. Didychuk AL, Butcher SE and Brow DA: The life of U6 small nuclear RNA, from cradle to grave. RNA 24: 437-460, 2018.
28. Sun M, Gao J, Meng T, Liu S, Chen H, Liu Q, Xing X, Zhao C and Luo Y: Cyclin G2 upregulation impairs migration, invasion, and network formation through RNF123/Dvl2/JNK signaling in the trophoblast cell line HTR8/SVneo, a possible role in preeclampsia. FASEB J 35: e21169, 2021.
29. Chen Q, Jiang S, Liu H, Gao Y, Yang X, Ren Z, Gao Y, Xiao L, Hu H, Yu Y, *et al*: Association of lncRNA SH3PXD2A-AS1 with preeclampsia and its function in invasion and migration of placental trophoblast cells. Cell Death Dis 11: 583, 2020.
30. Peng WX, Koirala P and Mo YY: LncRNA-mediated regulation of cell signaling in cancer. Oncogene 36: 5661-5667, 2017.
31. Yaghoobi A, Rezaee M, Behnoush AH, Khalaji A, Mafi A, Houjaghan AK, Masoudkabir F and Pahlavan S: Role of long noncoding RNAs in pathological cardiac remodeling after myocardial infarction: An emerging insight into molecular mechanisms and therapeutic potential. Biomed Pharmacother 172: 116248, 2024.
32. Balusu S, Horré K, Thrupp N, Craessaerts K, Snellinx A, Serneels L, T'Syen D, Chrysidou I, Arranz AM, Sierksma A, *et al*: MEG3 activates necroptosis in human neuron xenografts modeling Alzheimer's disease. Science 381: 1176-1182, 2023.
33. Guo J, Zheng W, Liu Y, Zhou M, Shi Y, Lei M, Zhang C and Liu Z: Long non-coding RNA DLX6-AS1 is the key mediator of glomerular podocyte injury and albuminuria in diabetic nephropathy by targeting the miR-346/GSK-3β signaling pathway. Cell Death Dis 14: 172, 2023.

34. Wang L, Shi L, Zhou B, Hong L, Gong H and Wu D: METTL3-mediated lncRNA HOXD-AS1 stability regulates inflammation, and the migration and invasion of trophoblast cells via the miR-135a/β-TRCP axis. Noncoding RNA Res 9: 12-23, 2023.
35. Tang X, Cao Y, Wu D, Sun L and Xu Y: Downregulated DUXAP8 lncRNA impedes trophoblast cell proliferation and migration by epigenetically upregulating TFPI2 expression. Reprod Biol Endocrinol 21: 58, 2023.
36. Dong N, Li D, Cai H, Shi L and Huang L: Expression of lncRNA MIR193BHG in serum of preeclampsia patients and its clinical significance. J Gynecol Obstet Hum Reprod 51: 102357, 2022.
37. Postepska-Igielska A, Giwojna A, Gasri-Plotnitsky L, Schmitt N, Dold A, Ginsberg D and Grummt I: LncRNA Khps1 regulates expression of the proto-oncogene SPHK1 via triplex-mediated changes in chromatin structure. Mol Cell 60: 626-636, 2015.
38. Xia K, Yu LY, Huang XQ, Zhao ZH and Liu J: Epigenetic regulation by long noncoding RNAs in osteo-/adipogenic differentiation of mesenchymal stromal cells and degenerative bone diseases. World J Stem Cells 14: 92-103, 2022.
39. Zhao S, Heng N, Weldegebriall Sahlu B, Wang H and Zhu H: Long noncoding RNAs: Recent insights into their role in male infertility and their potential as biomarkers and therapeutic targets. Int J Mol Sci 22: 13579, 2021.
40. Graf J and Kretz M: From structure to function: Route to understanding lncRNA mechanism. Bioessays 42: e2000027, 2020.
41. Niyaz M, Ainiwaer J, Abudureheman A, Zhang L, Sheyhidin I, Turhong A, Cai R, Hou Z and Awut E: Association between TP53 gene deletion and protein expression in esophageal squamous cell carcinoma and its prognostic significance. Oncol Lett 20: 1855-1865, 2020.
42. Zhang A, Xu M and Mo YY: Role of the lncRNA-p53 regulatory network in cancer. J Mol Cell Biol 6: 181-191, 2014.
43. Sharp AN, Heazell AE, Baczyk D, Dunk CE, Lacey HA, Jones CJ, Perkins JE, Kingdom JC, Baker PN and Crocker IP: Preeclampsia is associated with alterations in the p53-pathway in villous trophoblast. PLoS One 9: e87621, 2014.
44. Gao Q, Zhu X, Chen J, Mao C, Zhang L and Xu Z: Upregulation of P53 promoted G1 arrest and apoptosis in human umbilical cord vein endothelial cells from preeclampsia. J Hypertens 34: 1380-1388, 2016.
45. Fang Y, Zhang J, Zhu D, Mei Q, Liao T, Cheng H, He Y, Cao Y and Wei Z: MANF promotes unexplained recurrent miscarriages by interacting with NPM1 and downregulating trophoblast cell migration and invasion. Int J Biol Sci 20: 296-311, 2024.
46. Bao D, Zhuang C, Jiao Y and Yang L: The possible involvement of circRNA DMNT1/p53/JAK/STAT in gestational diabetes mellitus and preeclampsia. Cell Death Discov 8: 121, 2022.
47. Mo HQ, Tian FJ, Ma XL, Zhang YC, Zhang CX, Zeng WH, Zhang Y and Lin Y: PDIA3 regulates trophoblast apoptosis and proliferation in preeclampsia via the MDM2/p53 pathway. Reproduction 160: 293-305, 2020.
48. Liu C, Hu Y, Wang Z, Pan H, Ren Y, Li X, Liu Z and Gao H: The downregulation of placental lumican promotes the progression of preeclampsia. Reprod Sci 28: 3147-3154, 2021.
49. Qin G, Tu X, Li H, Cao P, Chen X, Song J, Han H, Li Y, Guo B, Yang L, *et al*: Long noncoding RNA p53-stabilizing and activating RNA promotes p53 signaling by inhibiting heterogeneous nuclear ribonucleoprotein K deSUMOylation and suppresses hepatocellular carcinoma. Hepatology 71: 112-129, 2020.
50. Chen Y, Hao Q, Wang S, Cao M, Huang Y, Weng X, Wang J, Zhang Z, He X, Lu H and Zhou X: Inactivation of the tumor suppressor p53 by long noncoding RNA RMRP. Proc Natl Acad Sci USA 118: e2026813118, 2021.
51. Song C, Xiong Y, Liao W, Meng L and Yang S: Long noncoding RNA ATB participates in the development of renal cell carcinoma by downregulating p53 via binding to DNMT1. J Cell Physiol 234: 12910-12917, 2019.
52. Tang R, Mei X, Wang YC, Cui XB, Zhang G, Li W and Chen SY: LncRNA GAS5 regulates vascular smooth muscle cell cycle arrest and apoptosis via p53 pathway. Biochim Biophys Acta Mol Basis Dis 1865: 2516-2525, 2019.
53. Li X, Zhao J, Geng J, Chen F, Wei Z, Liu C, Zhang X, Li Q, Zhang J, Gao L, *et al*: Long non-coding RNA MEG3 knockdown attenuates endoplasmic reticulum stress-mediated apoptosis by targeting p53 following myocardial infarction. J Cell Mol Med 23: 8369-8380, 2019.
54. Stein Y, Rotter V and Aloni-Grinstein R: Gain-of-function mutant p53: All the roads lead to tumorigenesis. Int J Mol Sci 20: 6197, 2019.
55. Vousden KH and Prives C: Blinded by the light: The growing complexity of p53. Cell 137: 413-431, 2009.